SIMULATION OF SEMICONDUCTOR DEVICES AND PROCESSES Vol. 4
Edited by W. Fichtner, D. Aemmer - Zurich (Switzerland) September 12-14, 1991 - Hartung-Gorre

Physical simulation of small-signal rate-dependent anomalies in GaAs MESFET's: a two-dimensional frequency-domain approach

Giovanni Ghione
Università di Catania, D.E.E.S.,
Viale Andrea Doria 6, 95121 Catania, Italy

Marco Pirola and Carlo U.Naldi
Politecnico di Torino, Dipartimento di Elettronica,
Corso Duca degli Abruzzi 24, 10129 Torino, Italy

Abstract

Rate-dependent anomalies such as the transconductance and output resistance low-frequency dispersion in GaAs MESFETs are analyzed through a frequency-domain, small-signal two-carrier drift-diffusion two-dimensional model accounting for the dynamic behaviour of deep levels and allowing for a backgate electrode. Results are discussed concerning the low-frequency dispersion of the small-signal parameters for MESFET epitaxial devices having deep substrate acceptor impurities or on semi-insulating intrinsic substrate, with or without backgating.

1 Introduction

The AC operation of GaAs MESFETs is affected by a number of rate-dependent anomalies leading to the so-called *low frequency dispersion* of some of the small-signal parameters [3, 4, 5, 7, 13]. These effects are connected to the dinamic behaviour of surface, substrate and interface deep-level traps (DLTs): while the DLT ionization is sensitive to DC bias, DLTs cease to react to AC driving signals beyond a certain frequency which commonly ranges from a few hundreds Hz to several KHz. A good understanding of this phenomenon is relevant to both the technological optimization and the modelling of GaAs MESFETs.

In fact, even if the dramatic DC hysteresis phenomena or slow transients observed in early MESFETs have been overcome owing to the improvement of substrate processing, rate-dependent effect still have a negative impact on device performance evaluation since they tend to mask the real (microwave or dynamic) behaviour of the device, which e.g. displays a far better DC output resistance and a slightly better DC transconductance than the actual microwave values. On the other hand, low-frequency dispersion also poses a modelling problem. Since many circuit-oriented MESFET models are based on a dual fitting strategy on experimental data, whereby part of the model (e.g. the drain current generator) is fitted on DC data, while other parameters (e.g. reactive elements) are fitted on AC measurements, large errors arise in modelling parameters such as the output resistance, which displays a DC value being as much as twice as the microwave value. Empirical circuit-oriented models have been proposed which are able to simulate this effect through the use of an RC feedback (cfr. e.g. the SPICE model presented in [14]); from the standpoint of physical modelling, it ought to be stressed that

substrate effects, however well understood and accurately included in the model, are bound to be critical when comparing simulation and experiment, owing to the great uncertainity of substrate data. In fact, the very characterization of bulk semi-insulating (S.I.) GaAs is far from being trivial [1, 15, 17], since the concentration of residual defects (C, EL1-EL6) is not accurately known prior to annealing, and, moreover, significantly changes during annealing [18]; for a more detailed discussion see [12].

In spite of the simple qualitative interpretation of rate-dependent phenomena as the effect of DLTs, a detailed understanding of the DLT frequency-dependent dynamics in realistic devices cannot be said to have been reached yet. Firstly, the role of surface and substrate DLTs still is controversial, and it is unclear when and under what conditions either kind can play a dominant role (see [4] and [20] for contrasting conclusions on this point). Secondly, several detailed mechanisms have been invoked to explain the dispersion of the output resistance through frequency-dependent substrate current injection, but their actual relevance has never been ascertained from a quantitative standpoint. Finally, the evidence brought forth in [20] suggests that the presence of a grounded *backgate electrode* can, under proper conditions, enhance rate-dependent substrate phenomena.

Majority-carrier DC models with partly ionized DLTs have been presented in [9, 10] and [2], while one- or two two-carrier time-domain large-signal models are discussed in [16], [20], respectively. Surface depletion effects have been included in several physical models appeared so far [3, 8, 11]; simplified *ad hoc* models can be found e.g. in [13].

While large-signal time-domain models are able to provide satisfactory insight on the slow trap dynamics, they cannot effectively and accurately correlate the low- and high-frequency behaviour of the small-signal parameters, owing to the widely different time constants involved. A small-signal frequency-domain approach is better suited to this aim. Although the small-signal frequency-domain simulation of DLTs dynamics has already been addressed in the domain of Si devices [6], a frequency-domain small-signal physical model including DLTs and backgating has never, as far as our knowledge goes, proposed for MESFET simulation.

In the present work, the simulation of rate-dependent effects in small-signal operation is addressed within the framework of a 2D physical two-carrier drift-diffusion model, including partly ionized shallow and deep levels. The paper is structured as follows. In Section 2 the DC and small-signal physical models are presented; Section 3 is devoted to a discussion and interpretation of results on the small-signal behaviour of MESFETs with deep substrate levels with or without backgate electrode, with particular attention to the low-frequency anomalies of the device admittance parameters.

2 The physical model

Although MESFETs behave as majority carrier devices in all operating conditions apart from breakdown, the effect of the hole density cannot be neglected in device structures including e.g. p-type substrates or substrates with undepleted p-type buried layers. A full steady-state two-carrier drift-diffusion model was therefore implemented to investigate DLT effects. Non-stationary effects, which are not included in the present model, are not expected to have significant interplay with the slow substrate phenomena addressed in the paper. The model equations read in steady-state DC conditions:

$$\nabla^2\phi = -\frac{q}{\epsilon_s}(p - n + \sum_j N_{Dj}^+ - \sum_i N_{Ai}^-) \tag{1}$$

$$\nabla \cdot \underline{J}_n = qR \tag{2}$$
$$\nabla \cdot \underline{J}_p = -qR \tag{3}$$

where:

$$\underline{J}_n = q[n\mu_n(\mathcal{E})\underline{\mathcal{E}} + D_n(\mathcal{E})\nabla n] \tag{4}$$
$$\underline{J}_p = q[n\mu_p(\mathcal{E})\underline{\mathcal{E}} - D_p(\mathcal{E})\nabla n] \tag{5}$$

are the electron and hole current densities, respectively. n is the electron density, p the hole density, $\underline{\mathcal{E}}$ the electric field, ϕ the potential, μ_n, μ_p, D_n, D_p the mobility and diffusivity of electrons and holes, respectively. The mobility-field curve of electrons is approximated as:

$$v(\mathcal{E}) = \mu_n(\mathcal{E})\mathcal{E} = \frac{\mu_i \mathcal{E} + v_s(\mathcal{E}/\mathcal{E}_t)^4}{1 + (\mathcal{E}/\mathcal{E}_t)^4}; \tag{6}$$

v_s is the saturation velocity, μ_i is the initial mobility, and $\mathcal{E}_t$ is related to the threshold field $\mathcal{E}_T$ as $\mathcal{E}_t = \mathcal{E}_T[3 - 4v_s/\mathcal{E}_T\mu_i]^{1/4}$. The hole mobility was taken as constant, and for both diffusivities Einstein relationship was assumed. N_{Dj}^+ is the density of the ionized j-th donor, N_{Ai}^- the density of the ionized i-th acceptor:

$$N_{Ai}^- = N_{Ai}\frac{c_{ni}n + c_{pi}n_i \exp(-a)}{c_{ni}[n + n_i \exp(a)] + c_{pi}[p + n_i \exp(-a)]} \tag{7}$$
$$N_{Dj}^+ = N_{Dj}\frac{c_{pj}p + c_{nj}n_i \exp(d)}{c_{nj}[n + n_i \exp(d)] + c_{pj}[p + n_i \exp(-d)]} \tag{8}$$

where:

$$a = \frac{\Delta E_V - E_g/2}{kT}, \qquad d = \frac{E_g/2 - \Delta E_C}{kT}; \tag{9}$$

E_g is energy gap of the material, k the Boltzmann constant, T the lattice temperature. Donor and acceptor levels are characterized by the concentration N_A or N_D, the activation energy, given by the energy difference between the impurity level and the bottom of the conduction band, ΔE_C, for donors, or by the energy difference between the impurity level and the top of the valence band, ΔE_V, for acceptors, and the capture probabilities c_n, c_p. The net electron generation-recombination (GR) rate R was characterized through a Shockley-Read-Hall model with a midgap center. This rather simplistic treatment is justified since in all cases of interest the hole current is virtually zero, thereby making the result independent of the detailed recombination mechanism.

Although surface traps are included into the model as an inhomogeneous, non-linear Neumann condition on Poisson's equation, the level ionization being treated as in (7), (8), the effect of surface trap dynamics on low-frequency dispersion of small-signal parameters, and its comparative importance with respect to substrate effects, will be addressed in a future paper.

Linearization around a working point of the time-domain two-carrier large-signal model and Fourier transformation, yields the following frequency-domain small-signal system:

$$\nabla^2 \delta\phi(\omega) = \frac{q}{\epsilon_s}\left(1 - \sum_j \frac{1}{1 + j\omega\tau_j}\frac{\partial N_{Dj}^+}{\partial n}\bigg|_0 + \sum_i \frac{1}{1 + j\omega\tau_i}\frac{\partial N_{Ai}^-}{\partial n}\bigg|_0\right)\delta n(\omega) +$$
$$+ \frac{q}{\epsilon_s}\left(-1 - \sum_j \frac{1}{1 + j\omega\tau_j}\frac{\partial N_{Dj}^+}{\partial p}\bigg|_0 + \sum_i \frac{1}{1 + j\omega\tau_i}\frac{\partial N_{Ai}^-}{\partial p}\bigg|_0\right)\delta p(\omega) \tag{10}$$

$$j\omega\delta n(\omega) + \nabla\cdot[(\mu_{n0}\mathcal{E}_0 + D_{n0}\nabla)\delta n(\omega) - n_0\tilde{\mu}\cdot\nabla\delta\phi(\omega)] = \left.\frac{\partial R}{\partial n}\right|_0 \delta n(\omega) + \left.\frac{\partial R}{\partial p}\right|_0 \delta p(\omega) \quad (11)$$

$$j\omega\delta p(\omega) + \nabla\cdot[(\mu_{p0}\mathcal{E}_0 - D_{p0}\nabla)\delta p(\omega) - p_0\mu_{p0}\nabla\delta\phi(\omega)] = -\left.\frac{\partial R}{\partial n}\right|_0 \delta n(\omega) - \left.\frac{\partial R}{\partial p}\right|_0 \delta p(\omega) \quad (12)$$

where $\delta\phi(\omega)$ is the Fourier transform of the small-signal potential, $\delta n(\omega)$ and $\delta p(\omega)$ are the Fourier transforms of the electron and hole small-signal densities, the subscript 0 refers to the bias point value, and the small-signal equivalent electron mobility tensor $\tilde{\mu}$ is defined as:

$$\tilde{\mu} = \mu_{n0}\left\{\mathbf{I} + \left.\frac{\partial\log(\mu_n)}{\partial\mathcal{E}}\right|_0 \left[\frac{(\mathcal{E}_0 + V_T\nabla\log(n_0))\mathcal{E}_0}{\mathcal{E}_0}\right]\right\} \quad (13)$$

where $V_T = kT/q$, the voltage equivalent of temperature. Finally, τ is the time constant of the donor or acceptor level, defined as:

$$\tau = \tau(n_0, p_0) = \frac{1}{c_{ni}[n_0 + n_i\exp(b)] + c_{pi}[p_0 + n_i\exp(-b)]} \quad (14)$$

where $b = a$ or $b = d$ for acceptor and donor levels, respectively. The frequency-dependent small-signal occupancy can be derived as e.g. in [6] from the rate equations for the level occupation probability.

The discretization of the DC model is performed by means of a mixed finite-boxes – finite-elements scheme on a triangular grid based on the Scharfetter-Gummel approach [19]. Details on the scheme as implemented in this work can be found in [11]; the DC solution is carried out through a coupled Newton technique. Some convergence problems have been experienced in the simulation of p-type substrates with deep acceptors; the numerical conditioning improves when accounting for recombination. Direct linearization of the discretized DC model around a working point is exploited for the frequency-domain small-signal analysis; for further details see [12].

3 Results and discussion

Rate-dependent mechanisms in MESFET's have been ascribed to the effect of either surface or substrate deep levels. In the present paper we shall confine ourselves to the discussion of substrate effects, with particular stress on backgate effects. The small-signal frequency-domain simulation allows to simply identify the cause of the low-frequency dispersion of input or output small-signal parameters without resorting to the cumbersome interpretation of large-signal transient data. As a case study, an epitaxial 1 μm MESFET has been analyzed, with a 0.2 μm uniformely doped ($N_D = 1\times10^{17}$ cm^{-3}) active layer; the gate width is normalized to 1 μm. In order to separate surface and substrate effects, in all simulations presented the surface potential has been set to zero. The device has been chosen so as to compare with the analyses reported in [20]. From this basic structure, four devices have been generated with different substrate properties. FET1a has a midgap (deep) acceptor both in the substrate and in the active layer, with concentration $N_A = 1\times10^{16}$ cm^{-3}; on the bottom of the substrate a backgate electrode is placed with a n-doped contact; the backgate doping is the same as in the active region, and the thickness of the n-doped backgate layer is 0.2 μm. FET1b is the same as FET1a, but the backgate electrode is left floating. FET1c has no backgate contact and the structure of FET1a. Finally, in FET2 deep acceptors are confined in the active region only, and no backgate is present. In all devices, a shallow donor also exists in the substrate with a

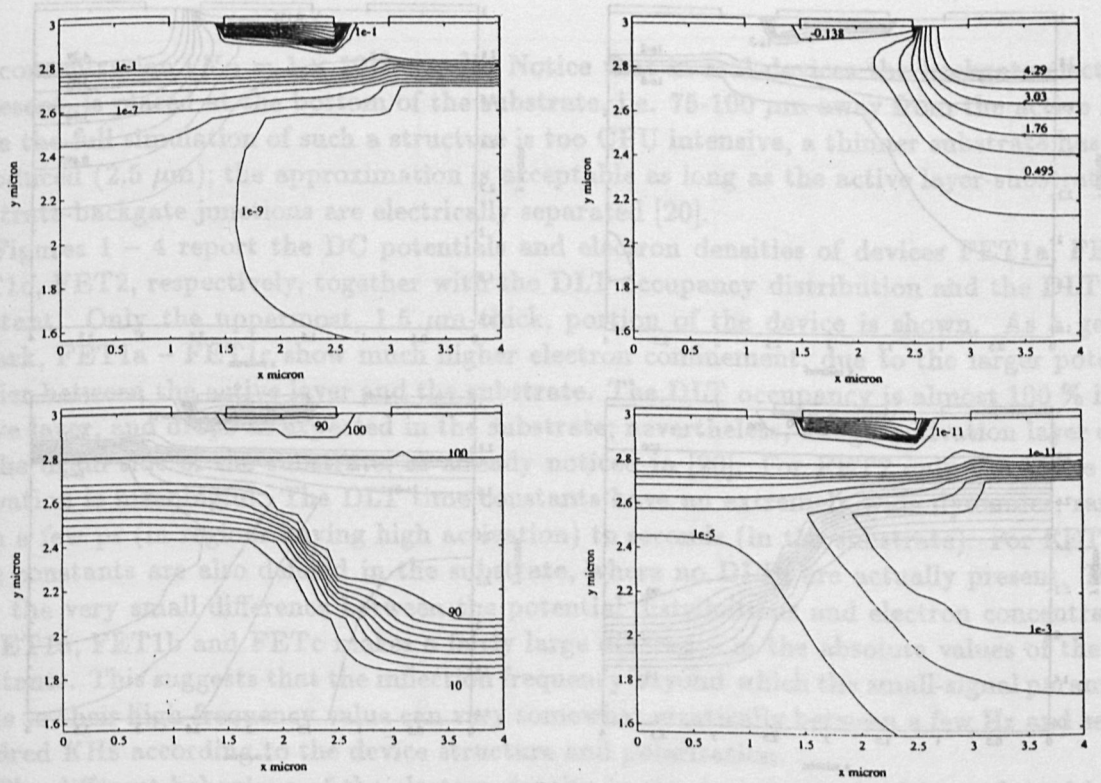

Figure 1: DC simulation of FET1a; the working point is $V_G = 0$ V, $V_D = 5$ V. From top row, left corner: electron concentration (10^{17} cm^{-3}), log scale; potential (V), linear scale; acceptor DLT % occupancy; DLT time constant (s), log scale.

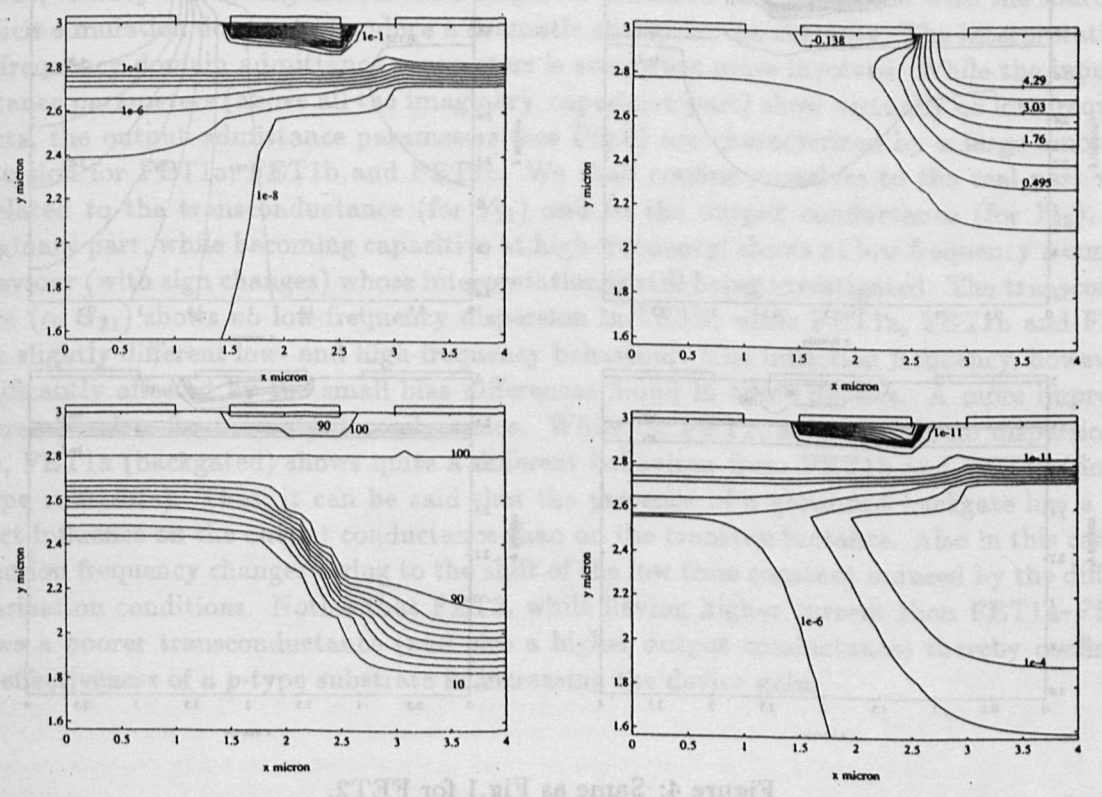

Figure 2: Same as Fig.1 for FET1b.

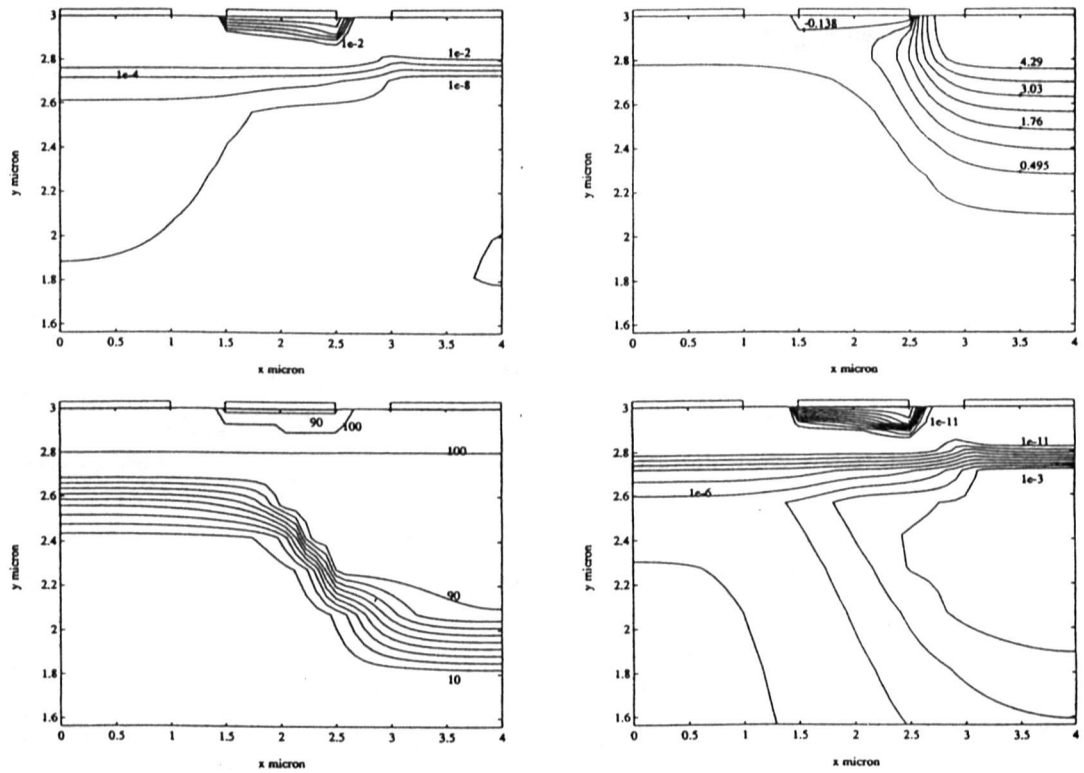

Figure 3: Same as Fig.1 for FET1c.

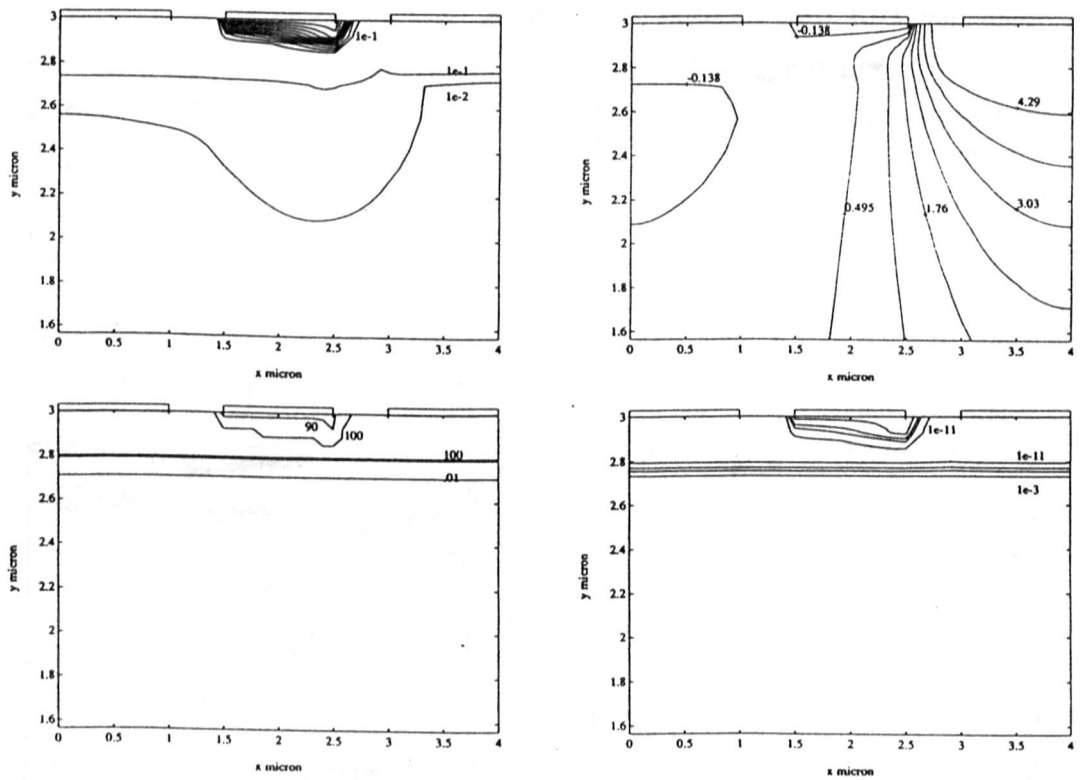

Figure 4: Same as Fig.1 for FET2.

low concentration ($N_D = 1 \times 10^{12}$ cm^{-3}). Notice that in real devices the backgate electrode, if present, is placed at the bottom of the substrate, i.e. 75-100 μm away from the active layer. Since the full simulation of such a structure is too CPU intensive, a thinner substrate has been introduced (2.5 μm); the approximation is acceptable as long as the active layer-substrate and substrate-backgate junctions are electrically separated [20].

Figures 1 – 4 report the DC potentials and electron densities of devices FET1a, FET1b, FET1c, FET2, respectively, together with the DLT occupancy distribution and the DLT time constant. Only the uppermost, 1.5 μm thick, portion of the device is shown. As a general remark, FET1a – FET1c show much higher electron confinement, due to the larger potential barrier between the active layer and the substrate. The DLT occupancy is almost 100 % in the active layer, and drops as expected in the substrate; nevertheless, a high activation layer exists on the drain side of the substrate, as already noticed in [20]. For FET2 only the active layer activation is meaningful. The DLT time constants have an extremely wide dynamics, ranging from a few ps (in regions having high activation) to seconds (in the substrate). For FET2 the time constants are also defined in the substrate, where no DLTs are actually present. Notice that the very small difference between the potential distributions and electron concentrations in FET1a, FET1b and FETc makes a fairly large difference in the absolute values of the time constants. This suggests that the inflection frequency beyond which the small-signal parameters settle to their high-frequency value can vary somewhat erratically between a few Hz and several hundred KHz according to the device structure and polarization.

The different behaviour of the electron density in the device examined is confirmed by the DC gate currents (Fig. 5) which are highest for the intrinsic device, while appear to be lowered by the effect of the p-type substrate. Little difference can be seen between FET1a, FET1b and FET1c, thereby confirming that, if the backgate is unbiased (i.e. connected with the source) its explicit simulation does not introduce a dramatic change in the currents. The interpretation of the frequency-domain admittance parameters is somewhat more involved. While the input admittance parameters (above all the imaginary, capacitive part) show virtually no low-frequency effects, the output admittance parameters (see Fig.6) are characterized by a large amount of dispersion for FET1a, FET1b and FET1c. We shall confine ourselves to the real part which is related to the transconductance (for Y_{21}) and to the output conductance (for Y_{22}). The imaginary part, while becoming capacitive at high frequency, shows at low frequency a complex behaviour (with sign changes) whose interpretation is still being investigated. The transconductance ($\approx G_{21}$) shows no low-frequency dispersion in FET2, while FET1a, FET1b and FET1c have slightly different low- and high-frequency behaviour. The inflection frequency, however, is significantly affected by the small bias differences found in these devices. A more impressive difference exists for the output conductance. While for FET2, as expected, no dispersion occurs, FET1a (backgated) shows quite a different behaviour from FET1b and FET1c (floating p-type substrate). Thus, it can be said that the presence of a grounded backgate has a more direct influence on the output conductance than on the transconductance. Also in this case the inflection frequency changes owing to the shift of the low time constant induced by the different polarization conditions. Notice that FET2, while having higher current than FET1a–FET1c, shows a poorer transconductance (and also a higher output conductance) thereby confirming the effectiveness of a p-type substrate in increasing the device gain.

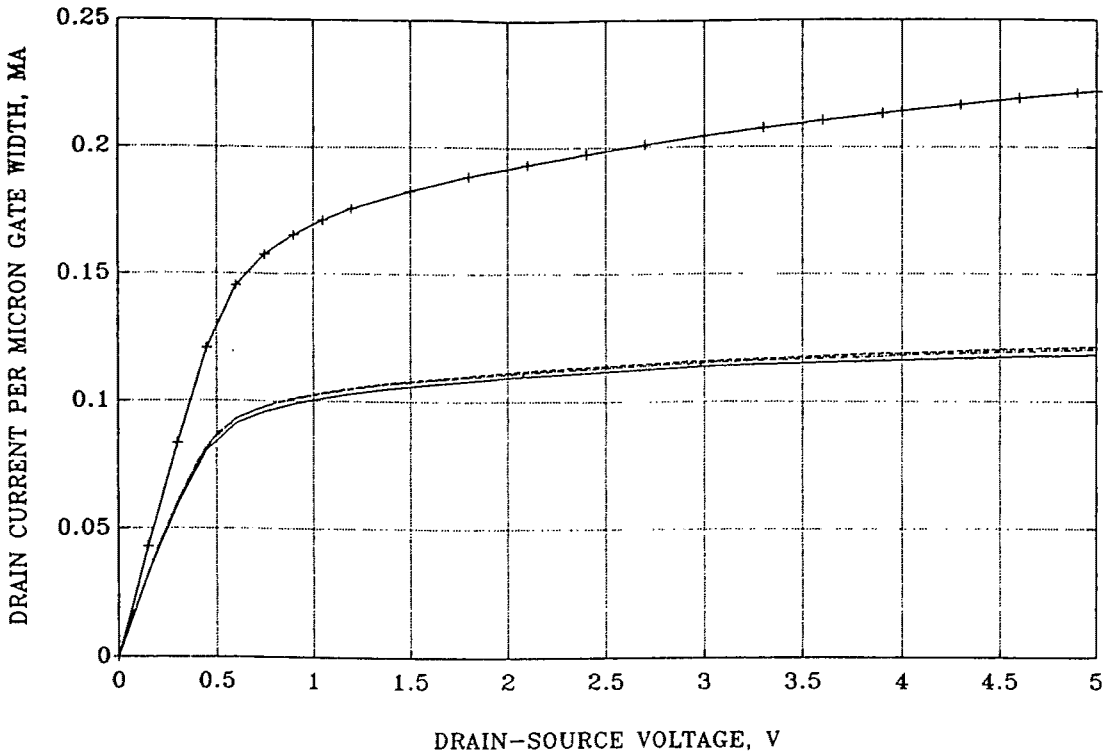

Figure 5: Drain current of FET1a (continuous curve), FET1b (dashed curve), FET1c (dashed-dotted curve), FET2 (continuous curve with crosses) for $V_g = 0$ V.

4 Conclusions

A small-signal frequency domain model has been discussed for the analysis of rate-dependent phenomena in GaAs MESFETs, with particular attention to the low-frequency dispersion of the small-signal parameters. Further work is being carried out to achieve a better understanding on the detailed dispersion mechanism, also correlating these with $1/f$ noise phenomena, and to gain deeper insight on the comparative importance of surface and substrate DLT-induced effects.

Aknowledgements. This work was partly supported by ALENIA, Roma. Helpful discussions with dr. A.Cetronio of ALENIA, Divisione Ricerche, are gratefully acknowledged.

References

[1] R.Anholt, T.W.Sigmon,M.D.Deal, "Process and devices models for GaAs MESFET technology", *Technical Digest of 1987 GaAs IC Symp.*, pp.53-56, Portland, Oct.1987.

[2] N. Araki-Mishima, K.Yamaguchi, "Two-Dimensional Numerical Analysis of GaAs MESFET's with a p-Buffer Layer", *Electronics and Communications in Japan*, Part 2, Vol.71, No.4, 1988, pp.19-25.

[3] T.M.Barton, C.M.Snowden, "Two-dimensional numerical simulation of trapping phenomena in the substrate of GaAs MESFETs", *IEEE Trans, on Electron Devices*, Vol. ED-37, N.6, pp.1409-1415, Jume 1990.

[4] T.M.Barton, P.H.Ladbrooke, "The role of the device surface in the high voltage behaviour of the GaAs MESFET", *Solid State Electronics*, Vol. 29, No. 8, pp.807-813, 1986.

[5] T.Ducourant, M.Rocchi, "Modelling of the drain lag effect in GaAs MESFET's and its impact on digital IC's", *Proceedings of ESSDERC '87*, Bologna, Sept. 1987, pp.313-316.

[6] A.Gnudi, P.Ciampolini, R.Guerrieri, M.Rudan, G.Baccarani, "Small-signal analysis of semiconductor devices containing generation-recombination centers", *Proc. of V NASECODE*, pp.207-212, Dublin, Ireland, June 1987.

[7] J.Graffeuil, Z.Hadjoub, J.P.Fortea, M.Pouysegur, "Analysis of capacitance and transconductance frequency dispersions in MESFET's for surface characterization", *Solid State Electronics*, Vol.29, No.10, pp.1087-1097, 1986.

[8] F.Heliodore, M.Lefebvre, G.Salmer, O.L.El-Sayed, "Two-dimensional simulation of submicrometer GaAs MESFET's: surface effects and optimization of recessed gate structures" *IEEE Trans. on Electron Devices*, vol. ED-35, No.7, pp.824-830, July 1988.

[9] K.Horio, Y.Fuseya, H.Kusuki, H.Yanai, "Numerical Simulation of GaAs MESFET's with a p-Buffer Layer on the Semi-Insulating Substrate Compensated by Deep Traps", *IEEE Trans. on Electron Devices*, vol. ED-37, No.9, pp.1371-1379, September 1989.

[10] K.Horio, K.Asada, H.Yanai, "Two-dimensional simulation of GaAs MESFETs with deep acceptors in the semi-insulating substrate", *Solid-State Eletronics*, Vol.34, No.4, pp.335-343, 1991.

[11] G.Ghione, C.U.Naldi, F.Filicori, M.Cipelletti, G.Locatelli, "MESS - A two dimensional physical device simulator and its application to the development of C-band power GaAs MESFETs", *Alta Frequenza*, Special Issue on Microwave CAD, Vol. LVII, N.7, pp.295-309, September 1988.

[12] G.Ghione, A.Benvenuti, M.Pirola, C.Naldi, " An extended majority-carrier approach for the DC and small-signal simulation of ion-implanted MESFET's on compensated and p-type substrates", *European Transactions on Telecommunications and Related Technologies*, Special Issue on Advanced Topics in Physical III-IV Device Simulation, Vol.1, N.4, July-August 1990, pp.411-419.

[13] P.H.Ladbrooke, S.R.Blight, "Low-field low-frequency dispersion of transconductance in GaAs MESFET's with implications for other rate-dependent anomalies", *IEEE Trans. on Electron Devices*, vol. ED-35, No.3, pp.257-267, March 1988.

[14] M.Lee, L.Forbes, T.Hallen, P.Tuinenga, "An analytical self-backgating GaAs MESFET model including deep-level trap effects", *Proceedings of IEDM-89*, pp.12.3.1-12.3.4, December 1989.

[15] K.Lehovec, R.Zuleeg, "Mobility, dopant and carrier distribution at the interface between semiconducting and semi-insulating gallium arsenide", in *Inst. Phys. Conf. Ser.* No. 24, Chapter 5, pp.292-306, 1975.

[16] S.H.Lo, C.P.Lee, "Two-dimensional simulation of the drain-current transient effect in GaAs MESFETs", *Solid-State Eletronics*, Vol.34, No.4, pp.397-401, 1991.

[17] M.Pillan, F.Vidimari, A.M.Orsucci, "Dependence of mobility profiles on doping transition and impurity concentration in GaAs FET structures", *Proc. 4th Conf. on Semi-insulating III-V Materials*, H.Kukimoto, ed., Ohmsha Ltd, Tokyo, May 1986.

[18] S.Reichlmaier, K.Löhnert, M.Baumgartner, "Undoped semi-insulating GaAs of very low residual acceptor concentration", *Japanese Journal of Applied Physics*, Vol.27, No.12, Dec. 1988, pp. 2329-2332.

[19] S.Selberherr, *Analysis and Simulation of Semiconductor Devices*, Springer Verlag, Wien 1984.

[20] I.Son, T.W. Tang, "modelling Deep-Level Trap Effects in GaAs MESFET's". *IEEE Trans. on Electron Devices*, vol. ED-36, No.4, p.632-640, April 1989.

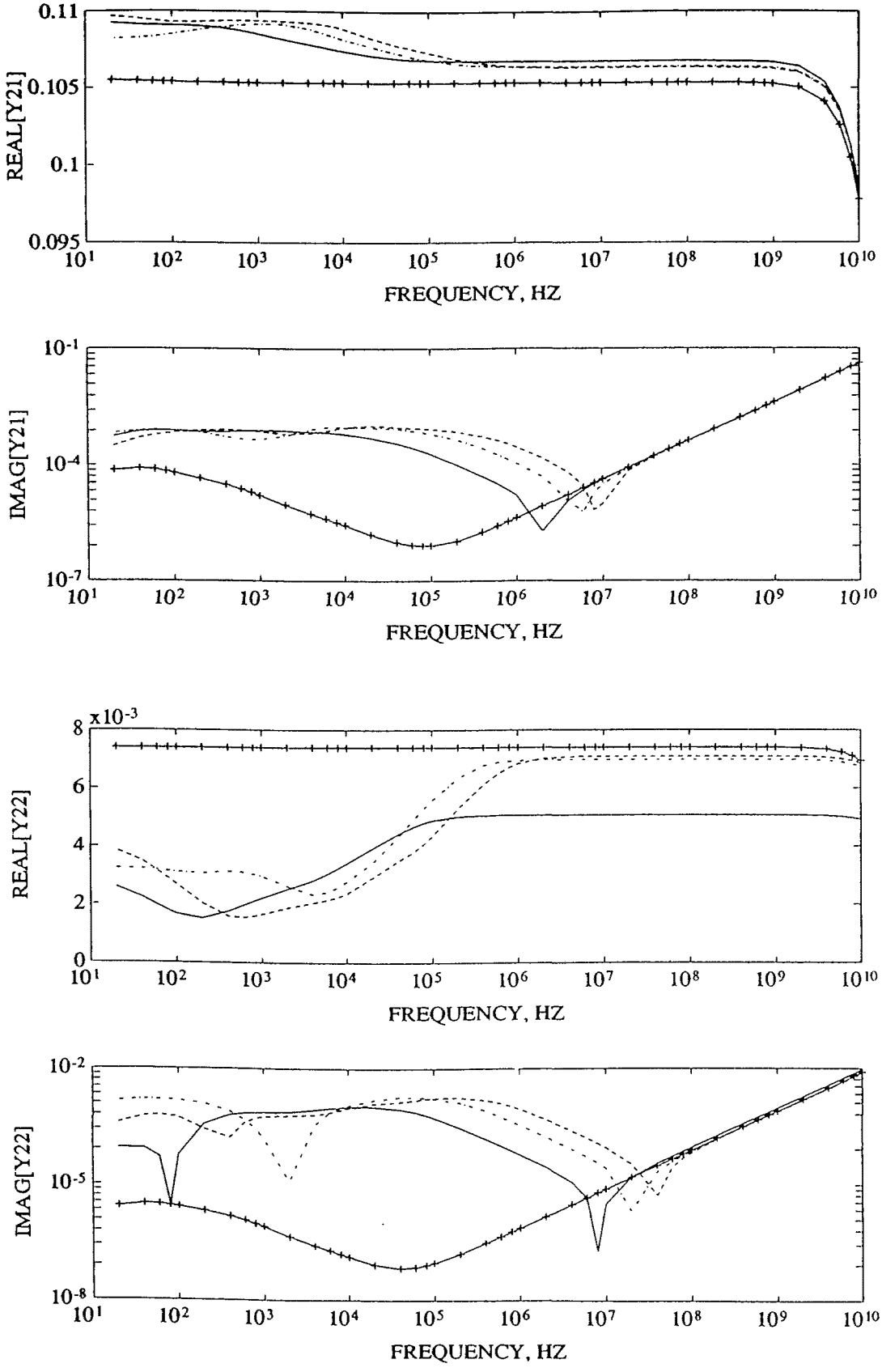

Figure 6: Output admittance parameters (mS) of FET1a, FET1b, FET1c, FET2 as a function of frequency. From top row: G_{21}, Abs(B_{21}) (log scale), G_{22}, Abs(B_{22}) (log scale). The same conventions as in Fig.5 are used.